Research Article

Pd(II), Cu(II), and pillared clay based nanocatalysts for low-temperature CO oxidation

Tatyana L. Rakitskaya[1] · Ganna M. Dzhyga[1] · Tatiana A. Kiose[1] · Liudmila P. Oleksenko[2] · Vitaliya Y. Volkova[1]

Abstract

Pillared clays (PILCs) are little-studied as supports in compositions of anchored metal complex catalysts. In the work, pillared clay, Al-PILC, was prepared by using Ukrainian natural bentonite, N-Bent, and the aluminum polycation, $[Al_{13}O_4(OH)_{24}(H_2O)_{12}]^{7+}$ (Al_{13}), as an intercalating agent. The final product was used for preparing K_2PdCl_4–$Cu(NO_3)_2$–KBr/Al-PILC nanocatalysts by an impregnation method. Initial N-Bent and Al-PILC as well as the nanocompositions based on them were characterized by XRD, FT-IR spectroscopy, DTG–DTA, water vapor adsorption, and pH metry. K_2PdCl_4–$Cu(NO_3)_2$–KBr/$\bar{S}$ compositions ($\bar{S}$ were N-Bent or Al-PILC) were tested in the reaction of CO oxidation with air oxygen at temperature of 20 °C and a relative humidity of 67%. It has been found that the preliminary modification of natural bentonite by Al_{13} intercalation results in formation of the nanostructured catalyst with a crystallite size of 19 nm showing the maximum activity in the reaction under study at $C_{Pd(II)} = 2.72 \times 10^{-5}$ mol/g and copper(II) concentrations of 2.9×10^{-5} and 5.9×10^{-5} mol/g.

Keywords Natural bentonite · Pillared clay · Nanocatalysts · Palladium(II) · Copper(II) · Carbon monoxide oxidation

1 Introduction

The fact that bentonites, both natural and modified, are widespread, inexpensive; available and environment-friendly sorbents permits to consider them as "materials of the twenty-first century" [1]. This denomination is confirmed by numerous studies concerning the synthesis of novel modified materials, particularly, pillared clays (PILCs) prepared by the polyhydroxy cation intercallation into montmorillonite and investigated from seventies of the last century [2]. Intercallation processes are very complicated and dependent on very many factors. Therefore, the repeatability of results and their comparison are hardly possible [3]. The properties of intercallation products depend on the nature of polyhydroxy cations (Al, Ti, Fe, Cr, Zn or Cu), synthesis conditions (concentration of metal polycations, hydrolysis, reaction time, washing, drying, and calcination), and, mainly, on origins of bentonites used [3, 4].

Pillared clays are prevalent as acid catalysts in organic synthesis and sorbents for both heavy metals and toxic gaseous substances [5–8]. Incorporation of transition metal ions into pillared clays extends the range of their application. These modified pillared clays are used as catalysts for oxidation of numerous organic compounds contained both in air and in aqueous solutions [2, 8–12] as well as for reduction of NO [7, 13, 14] and nitrate ions contained in water [15]. For the latter process, a Pd^0–Cu^0/Al-PILC catalyst was used. M/Al-PILC catalytic compositions (M is Cr, Cu or Ag) proposed for carbon monoxide oxidation [16, 17] are active only at high temperatures: t > 200 °C for Cu and Ag and t > 400 °C for Cr.

Pillared clays were not studied as supports for metal complex compounds which could be active at ambient temperatures in the reactions of deactivation of some

toxic gaseous substances, e.g. CO, SO$_2$, and O$_3$ [18–20]. As can be seen [18–24], anchored metal complex catalysts for CO oxidation necessarily contain palladium(II) and copper(II) compounds. Mainly, their catalytic activity can be improved by varying the support nature, the nature and concentrations of palladium(II) and copper(II) precursors, introduction of ligands, L, and by changing Pd(II):Cu(II):L ratio. As for halide ligands (L = Cl$^-$, Br$^-$, and I$^-$), palladium–copper complexes with bromide ligands demonstrated the maximum catalytic activity in the reaction of CO oxidation with air oxygen [18–20]. Our previous investigations [19, 20, 24] showed that chemical and phase compositions, structural, structural-adsorption, and physicochemical properties of natural minerals and their modified forms substantially influence the catalytic activity of palladium–copper complexes in the above-named reaction. For changing these properties of supports, different modification methods were used.

The aim of the current work was to synthesize nanosized pillared clay from one of Ukrainian bentonites and to evaluate the effect of this PILC on the activity of palladium–copper complexes supported on PILC in the reaction of carbon monoxide oxidation with air oxygen.

2 Experimental

Al-pillared clay was synthesized from natural bentonite (N-Bent) from Dashukovskii deposit (Ukraine) with the following chemical composition (wt%): SiO$_2$—50.60, Al$_2$O$_3$—15.58, Fe$_2$O$_3$—8.72, TiO$_2$—0.50, MgO—2.64, CaO—2.07, Na$_2$O—0.20, K$_2$O—0.05 by the known procedure [15] under the following conditions: an OH/Al molar ratio of 2.0, a bentonite content in aqueous suspension of 1.0 wt%, an Al content in bentonite of 20 mmol/g, calcination at 500 °C for 2 h.

K$_2$PdCl$_4$–Cu(NO$_3$)$_2$–KBr/$\bar{S}$ compositions ($\bar{S}$ is N-Bent or Al-PILC) were prepared by incipient wetness impregnation of each support with aqueous-alcohol solution at certain ratios of the above-named salts. The wet mass obtained was kept in a closed Petri dish at 20–25 °C for 24 h and then dried in an oven at 110 °C till constant weight. A palladium(II) content in the samples thus obtained was varied from 1.36×10^{-5} to 4.08×10^{-5} mol/g while a copper(II) content was varied from 1.17×10^{-5} to 8.8×10^{-5} mol/g; a KBr content for each sample was 1.02×10^{-4} mol/g. The catalyst samples were denoted as Pd(II)–Cu(II)/$\bar{S}$ ($\bar{S}$ is N-Bent or Al-PILC).

The X-ray diffraction powder analysis was carried out on a Siemens D500 diffractometer (CuK$_\alpha$ radiation, $\lambda = 1.54178$ Å) with a secondary beam graphite monochromator.

Analysis of FT-IR spectra in the range from 400 to 4000 cm^{-1} with resolution of 4 cm^{-1} was carried out using a Perkin Elmer FT-IR spectrometer. All spectra were recorded using pellets consisting of 1 mg of the material under study and 200 mg of KBr compressed under pressure of 7 tons/cm^2 for 30 s.

The thermal behavior of the samples (0.25 g each) was investigated by DTG–DTA using a Paulik, Paulik and Erdey derivatograph in the temperature range from 25 to 1000 °C with a linear heating rate of 10 °C/min. The measurement error was ± 5%.

Water vapor adsorption/desorption was studied gravimetrically using a vacuum setup temperature-controlled at 21 ± 0.2 °C containing a conventional McBain–Bakr silica-spring balance [25].

Protolytic properties of the bentonite surface were estimated by measurement of a pH equilibrium value in aqueous suspensions of 0.2 g N-Bent or Al-PILC in 20 mL of distilled water. pH values were measured by a pH-340 instrument with an ESL 43-07 glass electrode and an EVL 1M3 chlorsilver electrode under continuous stirring of the suspension at 20 °C.

The samples (1 g) of K$_2$PdCl$_4$–Cu(NO$_3$)$_2$–KBr/$\bar{S}$ compositions were tested in a gas-flow setup with a fixed-bed reactor at an initial CO concentration in the gas-air mixture (GAM), C_{CO}^{in}, of 300 mg/m^3 and also 50 mg/m^3 (see Fig. 6 and Table 3) and the following GAM parameters: temperature of 20 °C, relative humidity, φ_{GAM}, of 67%, a volume flow rate, w, of 1 L/min, a linear velocity, U, of 4.2 cm/s. As a result, an effective residence time, τ', was of 0.095 s. By monitoring final CO concentrations, C_{CO}^{f}, a carbon monoxide conversion in a steady state mode, η_{st} (%) was determined as the parameter characterizing the catalytic activity of the compositions.

3 Results and discussion

3.1 Phase composition

X-ray diffraction patterns for N-Bent, Al-PILC, and Pd(II)–Cu(II)/$\bar{S}$ at $C_{Pd(II)} = 2.72 \times 10^{-5}$ and $C_{Cu(II)} = 2.9 \times 10^{-5}$ mol/g are shown in Fig. 1. The concentrations of these metal ions were the same in all cases if not specified otherwise. After intercalation of the Al polyhydroxy cation, the montmorillonite, Mont (M in Fig. 1), and α-quarts. Q, phases remained in Al-PILC and Pd(II)–Cu(II)/Al-PILC samples whereas the calcite phase, C, disappeared. No additional reflection were detected in X-ray diffraction patterns 2 and 4 being evidence that initial crystalline Pd(II) and Cu(II) salts, oxide, PdO, CuO, or reduced, Pd^0 and Cu^0, forms were absent.

Fig. 1 X-ray diffraction patterns for N-Bent (1), Pd(II)–Cu(II)/N-Bent (2), Al-PILC (3), and Pd(II)–Cu(II)/Al-PILC (4) (M is montmorillonite, Q is α-quartz, and C is calcite)
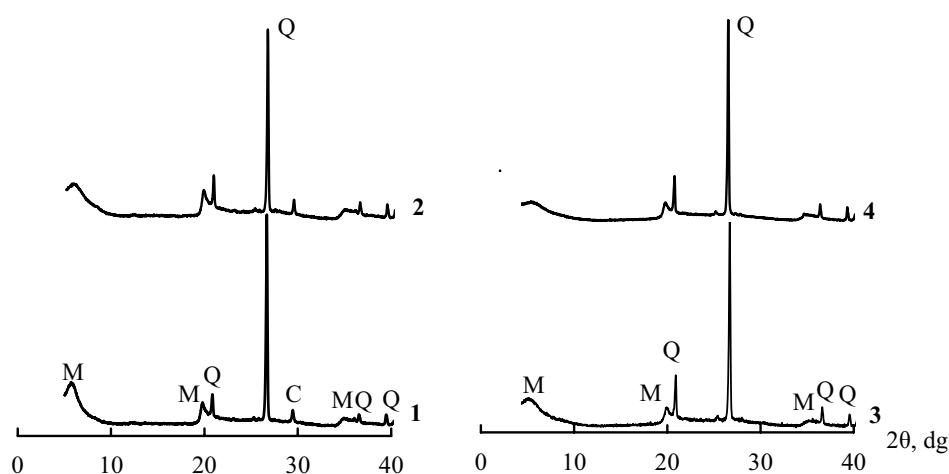

Table 1 X-ray diffraction parameters for N-Bent and Al-PILC as well as for Pd(II)–Cu(II) compositions based on them

Sample	2θ (°)	d_{001} (Å)	Δd (Å)	d_{060} (Å)	D (nm)
N-Bent	5.739	15.387	5.79	1.501	14
Pd(II)–Cu(II)/N-Bent	6.156	14.345	4.75	1.501	30
Al-PILC	5.088	17.354	7.75	1.503	18
Pd(II)–Cu(II)/Al-PILC	5.592	15.791	6.19	1.502	19

Catalyst components were homogenized over N-Bent and Al-PILC surfaces as palladium–copper complexes. Table 1 demonstrates the influence of Al polyhydroxy cation intercalation and active component anchoring on XRD parameters of supports and corresponding Pd(II)–Cu(II)/$\bar{S}$ catalyst samples. Taking into account d_{001} values and a thickness of the aluminosilicate pack (9.6 Å), we determined $\Delta d = d_{001} - 9.6$ Å characterizing an interlayer spacing. Δd Value was the highest for Al-PILC and interlayer spacings decrease in the order Al-PILC > Pd(II)–Cu(II)/Al-PILC > N-Bent > Pd(II)–Cu(II)/N-Bent. Intercalation of the Al_{13} polycation always results in expansion of aluminosilicate layers. However, according to some reported data, Δd values depend on the bentonite origin and intercalation conditions.

For instance, Δd values for Al-PILCs synthesized from Spanish bentonites were 9.4 Å [26] and 8.8 Å [27], while, for Turkish bentonites, those were 7.99 Å [28] and 8.9 Å [29]. Thus, our result is similar to that reported in [28]. The Al_{13} intercalation has no influence on the position of (060) reflection (Table 1) testifying that the crystalline structure of the aluminosilicate packs is not changed. After supporting palladium(II) and copper(II) compounds on Al-PILC the inter-pack space collapses that is consistent with some results reported elsewhere [2, 29]. However, in the case of Cu/Al-PILC containing 0.8 wt% of Cu, an expansion of the interlayer distances occurs [10]. The crystallite

size, D (nm), for N-Bent is lower than those for Al-PILC and Pd(II)–Cu(II)/$\bar{S}$.

3.2 FT-IR spectral investigations

Figure 2 shows FT-IR spectra for N-Bent, Al-PILC, and Pd(II)–Cu(II)/$\bar{S}$. The Al_{13} intercalation and metal salts anchoring for both supports result in some changes in their IR spectra. The number and positions of absorption bands in the IR spectrum for Pd(II)–Cu(II)/N-Bent do not change as compared with the IR spectrum for N-Bent whereas IR spectra for Al-PILC and Pd(II)–Cu(II)/Al-PILC substantially differ from the IR spectrum for N-Bent. As can be seen from Fig. 2, the absorption bands at 3692 cm^{-1} (assigned to stretching vibrations of M–OH structure groups (M is metal), at 876 cm^{-1}, and 915 cm^{-1} (assigned to deformation vibrations in Al–Fe^{3+}–OH and in Al–Al–OH structure groups, respectively), and at 1421 cm^{-1} (assigned to stretching vibrations in CO_3^{2-} ion) disappear; the absorption band at 3622 cm^{-1} (assigned to stretching vibrations in Si–(OH)–Al structure groups) is shifted to a high-frequency region by 15 cm^{-1} for Al-PILC and by 11 cm^{-1} for Pd(II)–Cu(II)/Al-PILC; the bands assigned to stretching and deformation vibrations of OH groups in water molecules are shifted to high-frequency region by 10 cm^{-1} and 13 cm^{-1}, respectively; in the range of Si–O–Si stretching vibrations, instead the shoulder at 1096 cm^{-1}, a clear band at 1047 cm^{-1} shifted to high-frequency range by 8 cm^{-1} as compared with N-Bent appears; the band of deformation vibrations in Si–O–Si fragments (468 cm^{-1}) is shifted by 6 cm^{-1}.

All these changes confirm the fact of successful completion of the intercalation process and the sharp profile of Si–O–Si band is a proof of the highly ordered pillar structure. The data obtained are in line with those reported for Al-PILC [27, 30]. For Pd(II)–Cu(II)/Al-PILC, the high-frequency shift ($\Delta v = +13$ cm^{-1}) of the absorption
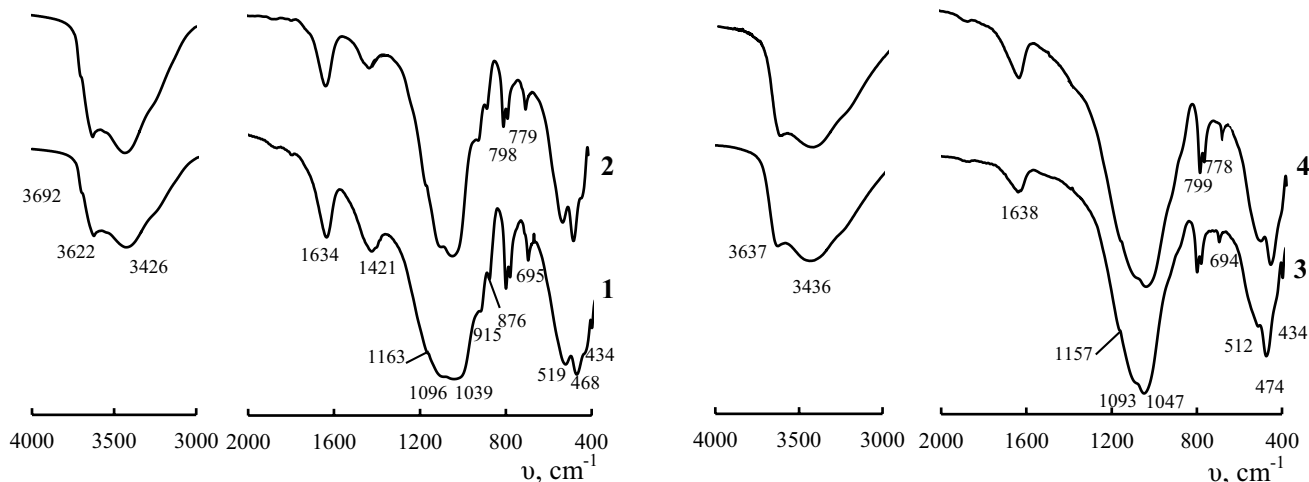
Fig. 2 FT-IR spectra for N-Bent (1), Pd(II)–Cu(II)/N-Bent (2), Al-PILC (3), and Pd(II)–Cu(II)/Al-PILC (4)
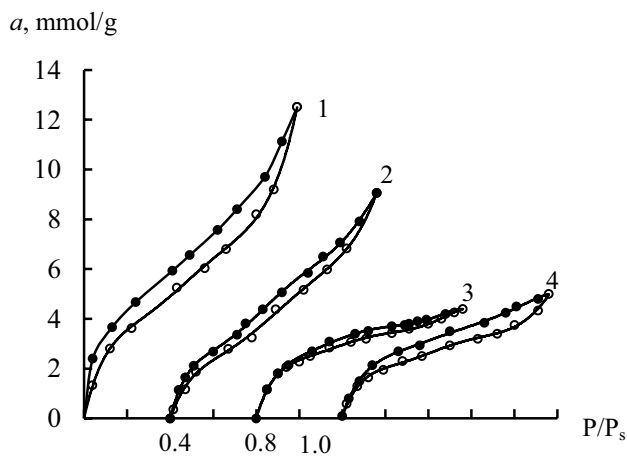

Fig. 3 Isotherms of water vapor adsorption(open circle)/desorption(black circle) by N-Bent (1), Pd(II)–Cu(II)/N-Bent (2), Al-PILC (3), and Pd(II)–Cu(II)/Al-PILC (4) (the isotherms are shifted relative to each other by 0.4 P/P_s)

band assigned to stretching vibrations of OH group in the associated water molecules shows that the palladium–copper complexes are anchored just on these sites.

3.3 Water vapor adsorption

The available data concerning water vapor adsorption by pillared clays are very scant [31, 32]. Our water vapor isotherms (Fig. 3) show that the adsorption by Al-PILC and Pd(II)–Cu(II)/Al-PILC is lower than for N-Bent and Pd(II)–Cu(II)/N-Bent.

Their hysteresis loops, especially for Al-PILC, are smaller in size and are closed at higher P/P_s values than the loop for N-Bent. These data are evidence of considerable structural changes in bentonite after Al_{13} intercalation.

Using the BET equation, we estimated the monolayer capacity. a_m, and the BET constant, C, characterizing the affinity between water molecules and the adsorbent surface. The heats of adsorption for the first layer, Q_1, and the specific surface areas, S_{sp}, were also evaluated using the known formulas [33]. The analysis of these parameters summarized in Table 2 shows that the intercalation and anchoring of palladium(II) and copper(II) compounds onto N-Bent and Al-PILC result in the decrease in a_m and S_{sp} values.

The water vapor adsorption isotherms were used for evaluation of a thermodynamic activity of adsorbed water, $a_{H_2O}=P/P_s$, that is an universal quantitative index considering structural and physicochemical properties of porous

Table 2 Structural-adsorption parameters and a thermodynamic activity of adsorbed water for N-Bent, Al-PILC and Pd(II)–Cu(II) compositions based on them

Sample	a_m (mmol/g)	C	Q_1 (J/mol)	S_{sp} (m²/g)	a_{H_2O}	
					a = 2.0 mmol/g	a = 4.0 mmol/g
N-Bent	3.11	32.78	8610	202	0.06	0.26
Pd(II)–Cu(II)/N-Bent	2.34	13.09	6422	152	0.14	0.46
Al-PILC	2.03	31.16	8542	132	0.13	0.86
Pd(II)–Cu(II)/Al-PILC	1.71	33.12	8691	111	0.19	0.86
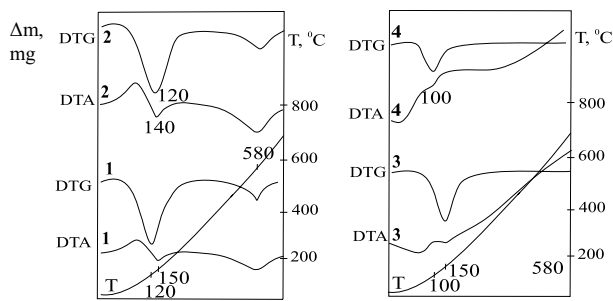
Fig. 4 Derivatograms for N-Bent (1), Pd(II)–Cu(II)/N-Bent (2), Al-PILC (3), and Pd(II)–Cu(II)/Al-PILC (4)

Fig. 5 Time dependences of pH values in aqueous suspensions of N-Bent (1) and Al-PILC (2)

sorbents, their geometric and energetic inhomogeneity [18]. For comparison of water activity values for different sorbents, they must be determined for the same adsorption value. a_{H_2O} Values presented in Table 2 were determined for a values of 2 mmol/g and 4 mmol/g. One can see that the minimal a_{H_2O} values were observed for N-Bent.

3.4 Thermochemical properties

As can be seen from thermochemical behavior of the two materials (Fig. 4), Al-PILC and Pd(II)–Cu(II)/Al-PILC, in contrast to N-Bent that demonstrates two endothermic effects, show a single endothermic effect which T_{M1} for Al-PILC is the same as that in the case of the first endothermic effect for N-Bent. The metal compounds anchored on Al-PILC decrease its T_M by 50 °C as compared with pure Al-PILC. The absence of the second endothermic effect (T_{M_2} = 580 °C) for Al-PILC and Pd(II)–Cu(II)/Al-PILC shows that all surface OH groups of bentonite were involved in the Al_{13} intercalation process.

3.5 Protolytic properties

It is known that the Pd^{2+} and Cu^{2+} aqua ions in aqueous medium can be hydrolyzed depending on pH [34]. The hydrolysis increases on the surface of porous supports [18, 35]. It is important to know how protolysis of water molecules occurs on acid (T^+) and basic (TO^-) surface sites

$$T^+ + HOH \leftrightarrow TOH + H^+,$$

$$TO^- + HOH \leftrightarrow TOH + OH^-,$$

and also about changes in pH level in aqueous suspensions of the samples under study. Time dependences of pH shown in Fig. 5 for N-Bent and Al-PILC suspensions show significant differences: pH equilibrium values for N-Bent and Al-PILC are 8.97 and 6.03, respectively.
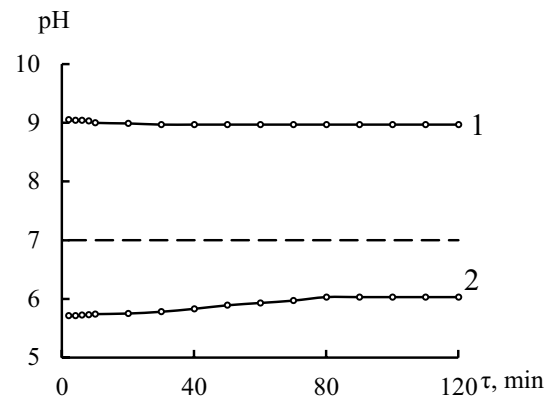
3.6 Pd(II)–Cu(II)/S̄ nanocomposition testing in the reaction of CO oxidation with air oxygen

Figure 6 shows time dependencies of a final carbon monoxide concentration, C_{Co}^f, for the reaction of CO oxidation by air oxygen over K_2PdCl_4–$Cu(NO_3)_2$–KBr/S̄ compositions (S̄ is N-Bent or Al-PILC). As can be seen, the modification of initial N-Bent by Al_{13} intercalation permits to prepare the Pd(II)–Cu(II)/Al-PILC nanocatalysts providing a steady state mode of CO oxidation as opposed to K_2PdCl_4–$Cu(NO_3)_2$–KBr/N-Bent composition for which C_{Co}^f increases with time and becomes equal to C_{Co}^{in} in 50 min.

Variation of Pd(II) concentration from 1.36×10^{-5} to 4.08×10^{-5} mol/g at $C_{Cu(II)} = 2.9 \times 10^{-5}$ mol/g and variation of Cu(II) concentration from 1.17×10^{-5} to 8.8×10^{-5} mol/g at $C_{Pd(II)} = 2.72 \times 10^{-5}$ mol/g showed that the maximum catalytic activity ($\eta_{st} = 33\%$) and the highest values of W_{in} (an initial reaction rate), W_{st} (a reaction rate in a steady state mode), k_I (a reaction rate constant calculated in the case of a steady state mode at an effective residence time, τ', of 0.095 s) were attained at $C_{Pd(II)} = 2.72 \times 10^{-5}$ mol/g and copper(II) concentrations of 2.9×10^{-5} and 5.9×10^{-5} mol/g (Table 3). Decreasing an initial CO concentration from 300 to 50 mg/m³ (Fig. 6), we obtained the similar values of k_I and η_{st}, that was evidence of the first-order reaction with respect to CO.

Based on the results of N-Bent, Al-PILC, and Pd(II)–Cu(II)/S̄ characterization, a conclusion can be drawn that the Al_{13} intercalation into the bentonite structure undoubtedly influence the activity of the nanocatalysts obtained. The changes in the bentonite structure, particularly, a Δd increase, for Al-PILC and Pd(II)–Cu(II)/Al-PILC (Table 1) cause a decrease in their pore-diffusion resistance and increase an access of CO molecules to active sites of the nanocatalyst. Despite the
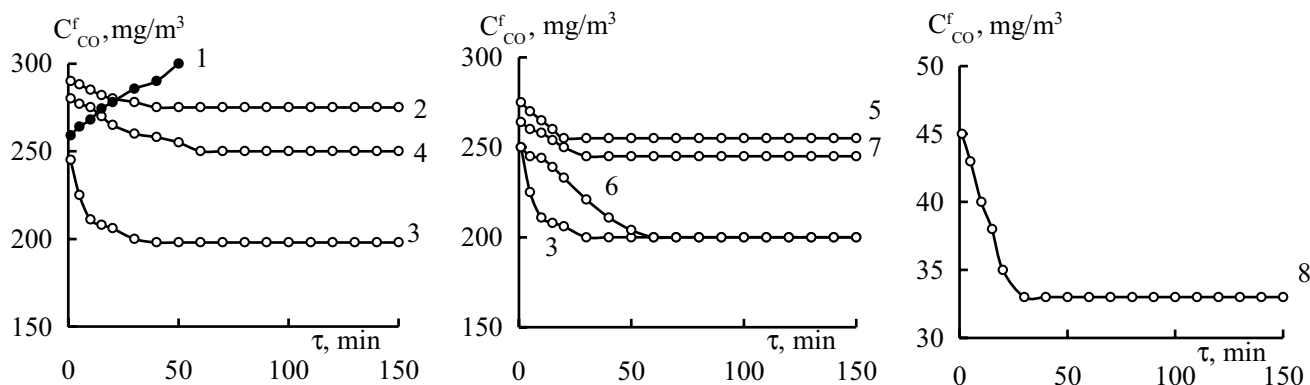
Fig. 6 Time dependences of C^f_{CO} for CO oxidation by air oxygen over K_2PdCl_4–$Cu(NO_3)_2$–KBr/$\bar{S}$ nanocompositions where $\bar{S}$: N-Bent (1) and Al-PILC (2–8). Experimental conditions including $C_{Pd(II)}$ and $C_{Cu(II)}$ are presented in Table 3

Table 3 Effect of palladium(II) and copper(II) concentrations in K_2PdCl_4–$Cu(NO_3)_2$–KBr/Al-PILC nanocatalysts on kinetic and stoichiometric parameters of the reaction of CO oxidation ($C_{KBr} = 1.02 \times 10^{-4}$ mol/g; U = 4.2 cm/s; $m_{cat} = 1$ g)

Numbers of curves in Fig. 6	$C_{Pd(II)} \times 10^5$ (mol/g)	$C_{Cu(II)} \times 10^5$ (mol/g)	$W \times 10^8$ (mol/(g s))		C^f_{CO} (mg/m^3)	k_I (s^{-1})	η_{st} (%)
			W_{in}	W_{st}			
K_2PdCl_4–$Cu(NO_3)_2$–KBr/N-Bent ($C^{in}_{CO} = 300$ mg/m^3)							
1	2.72	2.9	2.5	–	300	–	–
K_2PdCl_4–$Cu(NO_3)_2$–KBr/Al-PILC ($C^{in}_{CO} = 300$ mg/m^3)							
2	1.36	2.9	0.7	1.5	275	0.91	8
3	2.72	2.9	4.5	6.0	200	4.27	33
4	4.08	2.9	1.2	3.0	250	1.91	17
5	2.72	1.17	1.8	2.7	255	1.71	15
6	2.72	5.9	3.3	6.0	200	4.27	33
7	2.72	8.8	2.4	3.3	245	2.13	18
K_2PdCl_4–$Cu(NO_3)_2$–KBr/Al-PILC ($C^{in}_{CO} = 50$ mg/m^3)							
8	2.72	5.9	0.4	1.0	33	4.37	34

fact that S_{sp} for Pd(II)–Cu(II)/Al-PILC decreases (Table 2), this composition, as opposed to Pd(II)–Cu(II)/N-Bent, is characterized by clearly defined catalytic properties: the process of CO oxidation over this composition proceeds in a steady state mode (Fig. 6). Thus, a conclusion can be drawn that a S_{sp} value is not a critical factor influencing the catalytic activity of palladium–copper complexes anchored not only on Al-PILC but also on natural sorbents that has been shown in some our reports [18, 20, 23, 25]. Thermodynamic parameters of adsorbed water, particularly, a water activity and an ability of water molecules to protolytic dissociation depend on structural and physicochemical properties of a support. These thermodynamic parameters, by-turn, can influence the mechanism of surface complex formation and composition of palladium–copper complexes [18, 36].

As compared with N-Bent, in the case of Al-PILC, the Al_{13} intercalation results in increased a_{H_2O} (Table 2) and

decreased pH (down to 6.03) values measured in aqueous suspensions and the latter value indicates an increase in activity for hydronium ions (Fig. 5). Taking into consideration values of the first hydrolysis constants of palladium(II) and copper((II) i.e. pK(Pd^{2+}) = 2.0 and pK(Cu^{2+}) = 8.0 [34], one can come to a conclusion that Pd(II) and Cu(II) are hydrolyzed on the N-Bent surface whereas only Pd(II) is hydrolyzed on the Al-PILC surface. As can be seen from our investigations [18–20], in the latter case, the surface palladium–copper complexes formed are able to catalyze the reaction of CO oxidation with air oxygen. The maximum effect attained at certain contents of Pd(II) and Cu(II) (Fig. 6 and Table 3) is caused by synergy of their action [18].

4 Conclusions

Pillared clay used in the current study was prepared from Ukrainian bentonite by Al polyhydroxy cation (Al_{13}) intercalation. Nanosized pillared clay (D = 18 mm) and Pd(II)–Cu(II)/Al-PILC nanocatalysts (D = 19 mm) have been obtained. Though no change in crystalline structure for montmorillonite phase is observed, the interlayer spacings (in other words, "free space" between the aluminosilicate packs) for Al-PILC and Pd(II)–Cu(II)/Al-PILC are larger than those for N-Bent and Pd(II)–Cu(II)/N-Bent allowing easier access for CO molecules to active sites of the nanocatalyst. Active components of Pd(II)–Cu(II)/$\bar{S}$ compositions ($\bar{S}$ is N-Bent or Al-PILC) are not transformed to oxides or reduced forms, on the contrary, they are anchored on the support surface as palladium–copper complexes. Their compositions depend on some thermodynamic parameters of a certain support i.e. a thermodynamic activity of adsorbed water, a_{H_2O}, and hydronium ion activity, $a_{H_3O^+}$. Substantial differences in these parameters results in hydrolysis of both palladium(II) and copper(II) on the N-Bent surface ($a_{H_2O} = 0.46$ and pH 8.97) whereas only Pd(II) is hydrolyzed on the Al-PILC surface ($a_{H_2O} = 0.86$ and pH 6.03). These combinations of Pd(II) and Cu(II) forms of existence on the Al-PILC surface leads to appearance of their catalytic activity and synergistic effect at $C_{Pd(II)} = 2.72 \times 10^{-5}$, $C_{Cu(II)}$ of 2.9×10^{-5} and 5.9×10^{-5}, and $C_{KBr} = 1.02 \times 10^{-4}$ mol/g.

Compliance with ethical standards

Conflict of interest The authors declare that they have no conflict of interest.

References

1. Bergaya F, Lagaly G (2006) General introduction: clays, clay minerals, and clay science. In: Bergaya F, Theng BKG, Lagaly G (eds) Handbook of clay science, vol 1. Developments in clay science. Elsevier, Amsterdam, pp 1–18. https://doi.org/10.1016/S1572-4352(05)01001-9
2. Bahranowski K, Kielski A, Serwicka EM, Wisła-Walsh E, Wodnicka K (2000) Influence of doping with copper on the texture of pillared montmorillonite catalysts. Microporous Mesoporous Mater 41:201–215. https://doi.org/10.1016/S1387-1811(00)00294-8
3. Bineesh KV, Cho DR, Kim SY, Jermy BR, Park DW (2008) Vanadia-doped titania-pillared montmorillonite clay for the selective catalytic oxidation of H_2S. Catal Commun 9:2040–2043. https://doi.org/10.1016/j.catcom.2008.03.048
4. Cool P, Vansant EF (1998) Pillared clays: preparation, characterization and applications. In: Karge HG, Weitkamp J (eds) Synthesis, vol 1. Springer, Berlin, pp 265–288. https://doi.org/10.1007/3-540-69615-6_9
5. Figueras F (1988) Pillared clays as catalysts. Catal Rev Sci Eng 30:457–499. https://doi.org/10.1080/01614948808080811
6. Gil A, Gandía LM, Vicente MA (2000) Recent advances in the synthesis and catalytic applications of pillared clays. Catal Rev Sci Eng 42:145–212. https://doi.org/10.1081/CR-100100261
7. Ding Z, Kloprogge JT, Frost RL, Lu GQ, Zhu HY (2001) Porous clays and pillared clays-based catalysts. Part 2: a review of the catalytic and molecular sieve applications. J Porous Mater 8:273–293. https://doi.org/10.1002/chin.200219248
8. Baloyi J, Ntho T, Moma J (2018) Synthesis and application of pillared clay heterogeneous catalysts for wastewater treatment: a review. RSC Adv 8:5197–5211. https://doi.org/10.1039/c7ra12924f
9. Carriazo JG, Guelou E, Barrault J, Tatibouët JM, Moreno S (2003) Catalytic wet peroxide oxidation of phenol over Al–Cu or Al–Fe modified clays. Appl Clay Sci 22:303–308. https://doi.org/10.1016/S0169-1317(03)00124-8
10. Kim SC, Lee DK (2004) Preparation of Al–Cu pillared clay catalysts for the catalytic wet oxidation of reactive dyes. Catal Today 97:153–158. https://doi.org/10.1016/j.cattod.2004.03.066
11. Ksontini N, Najjar W, Ghorbel A (2008) Al–Fe pillared clays: synthesis, characterization and catalytic wet air oxidation activity. J Phys Chem Solids 69:1112–1115. https://doi.org/10.1016/j.jpcs.2007.10.069
12. Oliveira LCA, Lago RM, Fabris JD, Sapag K (2008) Catalytic oxidation of aromatic VOCs with Cr or Pd-impregnated Al-pillared bentonite: byproduct formation and deactivation studies. Appl Clay Sci 39:218–222. https://doi.org/10.1016/j.clay.2007.06.003
13. Chmielarz L, Kuśtrowski P, Zbroja M, Rafalska-Łasocha A, Dudek B, Dziembaj R (2003) SCR of NO by NH_3 on alumina or titania-pillared montmorillonite various modified with Cu or Co: part I. General characterization and catalysts screening. Appl Catal B 45:103–116. https://doi.org/10.1016/S0926-3373(03)00121-8
14. Yang RT, Chen JP, Kikkinides ES, Cheng LS, Cichanowicz JE (1992) Pillared clays as superior catalysts for selective catalytic reduction of nitric oxide with ammonia. Ind Eng Chem Res 31:1440–1445. https://doi.org/10.1021/ie00006a003
15. Rao GR, Mishra BG (2007) Al-pillared clay supported CuPd catalysts for nitrate reduction. J Porous Mater 14:205–212. https://doi.org/10.1007/s10934-006-9025-y
16. Tomul F, Balci S (2009) Characterization of Al, Cr-pillared clays and CO oxidation. Appl Clay Sci 43:13–20. https://doi.org/10.1016/j.clay.2008.07.006
17. Basoglu FT, Balci S (2016) Catalytic properties and activity of copper and silver containing Al-pillared bentonite for CO oxidation. J Mol Struct 1106:382–389. https://doi.org/10.1016/j.molstruc.2015.10.072
18. Rakitskaya TL, Ennan AA, Volkova VY (2005) Low-temperature catalytic air purification from carbon monoxide. Ekologiya, Odessa
19. Rakitskaya TL, Kiose TA, Zryutina AM, Gladyshevskii RE, Truba AS, Vasylechko VO, Demchenko PYu, Gryschouk GV, Volkova VY (2013) Solid-state catalysts based on bentonites and Pd(II)–Cu(II) complexes for low-temperature carbon monoxide oxidation. Solid State Phenom 200:299–304. https://doi.org/10.4028/www.scientific.net/ssp.200.299
20. Rakitskaya TL, Kiose TA, Golubchik KO, Ennan AA, Volkova VY (2017) Acid-modified clinoptilolite as a support for palladium–copper complexes catalyzing carbon monoxide oxidation with air oxygen. Chem Cent J 11:28. https://doi.org/10.1186/s13065-017-0256-6

21. Wang Y, Shi J, Wu R, Li X, Zhao Y (2016) Room-temperature CO oxidation over calcined Pd–Cu/palygorskite catalysts. Appl Clay Sci 119:126–131. https://doi.org/10.1016/j.clay.2015.08.034

22. Titov DN, Ustyugov AV, Tkachenko OP, Kustov LM, YaV Z, Veligzhanin AA, Sadovskaya NV, Oshanina IV, Bruk LG, Temkin ON (2012) State of active components on the surface of the $PdCl_2$–$CuCl_2$/γ-Al_2O_3 catalyst for the low temperature oxidation of carbon monoxide. Kinet Catal 53:262–273. https://doi.org/10.1134/s0023158412020140

23. Rakitskaya TL, Kiose TA, Golubchik KO, Dzhiga GM, Ennan AA, Volkova VY (2018) Catalytic compositions based on chlorides of d-metals and natural aluminosilicates for the low-temperature sulfur dioxide oxidation with air oxygen. Acta Phys Pol A 133:1074–1078. https://doi.org/10.12693/aphyspola.133.1074

24. Rakitskaya TL, Kiose TA, Golubchik KO (2015) Effect of tripoli phase composition on the activity of palladium–copper catalyst for carbon monoxide oxidation. Ukr Chem J 81:11–17

25. Rakitskaya TL, Truba AS, Ennan AA, Dlubovskii RM, Volkova VY (2017) Water vapor adsorption by nanostructured polyphase compositions based on the solid component of welding aerosol. Adsorpt Sci Technol 35:389–395. https://doi.org/10.1177/0263617416688691

26. Sánchez A, Montes M (1998) Influence of the preparation parameters (particle size and aluminium concentration) on the textural properties of Al-pillared clays for a scale-up process. Microporous Mesoporous Mater 21:117–125. https://doi.org/10.1016/s1387-1811(97)00057-7

27. Salerno P, Asenjo MB, Mendioroz S (2001) Influence of preparation method on thermal stability and acidity of Al-PILCs. Thermochim Acta 379:101–109. https://doi.org/10.1016/S0040-6031(01)00608-6

28. Altunlu M, Yapar S (2007) Effect of OH^-/Al^{3+} and Al^{3+}/clay ratios on the adsorption properties of Al-pillared bentonites. Colloids Surf A 306:88–94. https://doi.org/10.1016/s1387-1811(97)00057-7

29. Basoglu FT, Balci S (2010) Micro-mesopore analysis of Cu^{2+} and Ag^+ containing Al-pillared bentonite. Appl Clay Sci 50:73–80. https://doi.org/10.1016/j.clay.2010.07.004

30. Tomul F, Balci S (2007) Synthesis and characterization of Al-pillared interlayered bentonites. GUIS 21:21–31

31. Gruszkiewicz MS, Simonson JM, Burchell TD, Cole DR (2005) Water adsorption and desorption on microporous solids at elevated temperature. J Therm Anal Calorim 81:609–615. https://doi.org/10.1007/s10973-005-0832-1

32. Ng EP, Mintova S (2008) Nanoporous materials with enhanced hydrophilicity and high water sorption capacity. Microporous Mesoporous Mater 114:1–26. https://doi.org/10.1016/j.micromeso.2007.12.022

33. Gregg SJ, Sing KSW (1982) Adsorption, surface area and porosity. Academic Press, London. https://doi.org/10.1002/bbpc.19820861019

34. Baes CF, Mesmer RE (1976) The hydrolysis of cations. Wiley, New York. https://doi.org/10.1002/bbpc.19770810252

35. Tarasevich YI, Ovcharenko FD (1988) Structure and surface chemistry of laminar silicates. Naukova dumka, Kiev

36. Rakitskaya TL, Truba AS, Kiose TA, Raskola LA (2015) Mechanisms of d metal complex formation on porous supports and their catalytic activity in redox reactions. ONU Herald Chem 20:27–48. https://doi.org/10.18524/2304-0947.2015.2(54).50626